

RESEARCH ARTICLE

# Analytical expression of motion profiles with elliptic jerk

Daniele Stretti<sup>1</sup>, Pietro Fanghella<sup>2</sup>, Giovanni Berselli<sup>2</sup> and Luca Bruzzone<sup>2,\*</sup> 

<sup>1</sup>Magnet & Systems Unit, ASG Superconductors SpA, Genoa, Italy and <sup>2</sup>Department of Mechanical, Energy, Management and Transport Engineering (DIME), University of Genoa, Genoa, Italy

\*Corresponding author. E-mail: [luca.bruzzone@unige.it](mailto:luca.bruzzone@unige.it)

**Received:** 12 January 2023; **Revised:** 9 February 2023; **Accepted:** 15 February 2023; **First published online:** 10 March 2023

**Keywords:** motion control, elliptic jerk, motion profiles, vibrations

## Abstract

The paper discusses the analytical expressions of a motion profile characterized by elliptic jerk. This motion profile is obtained through a kinematic approach, defining the jerk profile and then obtaining acceleration, velocity, and displacement laws by successive integrations. A dimensionless formulation is adopted for the sake of generality. The main characteristics of the profile are analyzed, outlining the relationships between the profile parameters. A kinematic comparison with other motion laws is carried out: trapezoidal velocity, trapezoidal acceleration, cycloidal, sinusoidal jerk, and modified sinusoidal jerk. Then, the features of these motion profiles are evaluated in a dynamic case study, assessing the vibrations induced to a second-order linear system with different levels of damping. The results show that the proposed motion law provides a good compromise between different performance indexes (settling time, maximum absolute values of velocity and acceleration).

## 1. Introduction

The study on novel motion profiles is a motivating and valuable research area, since it can provide productivity increase and other significant benefits and to a wide variety of industrial applications. As a matter of fact, in many automation tasks transfer time represents a large part of the complete cycle time; as a consequence, the reduction of the transfer time can remarkably improve the overall plant efficiency. An emblematic example is robotics. Nowadays, robot mechanisms are much more lightweight and, consequently, flexible than in the past [1, 2], in particular when compliant joints are adopted [3, 4]. Therefore, the conception of smooth motion profiles, suitable for reducing residual vibrations and overshoot, plays a noteworthy role in the optimization of the task execution [5].

For given limits on force/torque and on linear/angular velocity, the motion completion time is minimized by trapezoidal velocity motion profiles, with constant acceleration and deceleration in the first and last phase, and constant velocity in the intermediate phase. Nevertheless, it is well known that this law, characterized by discontinuities in acceleration (infinite jerk), produces persistent residual vibrations, penalizing the settling time [6]. To face this issue, great research efforts have been devoted to the conception of smoother velocity profiles, which are frequently based on trigonometric or polynomials functions [7–11].

There are two main classes of methods which can be used for the generation of a rest-to-rest motion profile for a dynamic system.

The first class is represented by dynamic methods [12]. These approaches exploit the dynamic model of the system, optimizing the motion profile while respecting kinematic and dynamic constraints, such as limits on force/torque and on the jerk.

On the contrary, kinematic methods do not consider the dynamic model. The synthesis of the motion profile is based exclusively on kinematic assumptions and constraints, usually expressed in terms of acceleration and jerk [13]. Unquestionably, these methods are much simpler than dynamic ones, and

consequently, they are widespread in industry. Moreover, they are more suitable for all implementations in which the motion planning is not known a priori but needs to be calculated in real-time. On the other hand, only sub-optimal solutions can be obtained using kinematic methods, reducing the system's performance. However, reasonably good performances can be achieved, provided that jerk is properly limited [14].

In ref. [15], a kinematic method based on a motion law with elliptic jerk has been proposed and compared to other profiles discussed in the scientific literature: trapezoidal velocity, S-curve (trapezoidal acceleration), cycloidal, sinusoidal jerk [16], modified sinusoidal jerk [17].

The conception of this law is indeed curiosity-driven: the ellipse is a geometrical entity related to many physical phenomena, and it can be defined by a small number of parameters. Therefore, the starting point is the idea of defining a motion law with an elliptical jerk profile and then evaluating its features by comparison with other widely used and well-known profiles.

In this paper, the definition of the motion profile is presented (Section 2); then, the analytical expressions of jerk (Section 3.1), acceleration (Section 3.2), velocity (Section 3.3), and position (Section 3.4) are discussed. Section 3.5 explains how all the profile parameters can be calculated from a minimum set of independent parameters (six time parameters for the asymmetric elliptic jerk profile and four time parameters for the symmetric elliptic jerk profile). In Section 4, a purely kinematic comparison with the other considered motion profiles is carried out, in terms of coefficients of jerk, acceleration, and velocity. Then in Section 5, the comparison is extended using a dynamic model, assessing the vibrations induced by the motion profiles to a second-order linear system. In Section 6, conclusions are debated, outlining benefits and drawbacks of the proposed motion law.

The main novelty of the work with respect to the early results presented in ref. [15] is the presentation of the analytical expressions of the motion profile in terms of acceleration, velocity, and displacement, obtained by successive integrations, and a more extended discussion of the dynamic response as a function of the system damping coefficient.

## 2. Elliptic jerk motion profile

A dimensionless formulation is adopted for the sake of generality. For given displacement length  $h$  and motion duration  $T$ :

- the *dimensionless time* is the time  $t$  normalized by  $T$ :  $t_{ad} = t/T$ ;
- the *dimensionless position* is the position  $s$  normalized by  $h$ :  $s_{ad} = s/h$ ;
- the *dimensionless velocity* is the velocity  $v$  normalized by  $h/T$ :  $v_{ad} = vT/h$ ;
- the *dimensionless acceleration* is the acceleration  $a$  normalized by  $h/T^2$ :  $a_{ad} = aT^2/h$ ;
- the *dimensionless jerk* is the jerk  $j$  normalized by  $h/T^3$ :  $j_{ad} = jT^3/h$ .

The proposed motion law is based on the jerk profile shown in Fig. 1 as a function of the dimensionless time, which varies from 0 to 1 from rest to rest. This profile is divided into seven phases (#1–#7, Fig. 1). The  $i$ th phase starts at  $t_{ad,i-1}$  and ends at  $t_{ad,i}$ .

The first three phases are characterized by positive acceleration and have an overall duration  $t_{ad,pa}$ . The fourth phase has null acceleration and constant velocity. The last three phases are characterized by negative acceleration and have an overall duration  $t_{ad,na}$ . Consequently, the duration of the fourth phase is  $(1 - t_{ad,pa} - t_{ad,na})$ .

The positive acceleration motion is performed with positive jerk in phase #1, with null jerk in phase #2, and with negative jerk in phase #3. The durations of the phases #1 and #3 are, respectively,  $t_{ad,paj}$  and  $t_{ad,panj}$ . Consequently, the duration of phase #2 is  $(t_{ad,pa} - t_{ad,paj} - t_{ad,panj})$ .

The deceleration is performed with negative jerk in phase #5, with null jerk in phase #6, and with positive jerk in phase #7. The durations of the phases #5 and #7 are, respectively,  $t_{ad,nanj}$  and  $t_{ad,napj}$ . Consequently, the duration of phase #6 is  $(t_{ad,na} - t_{ad,nanj} - t_{ad,napj})$ .

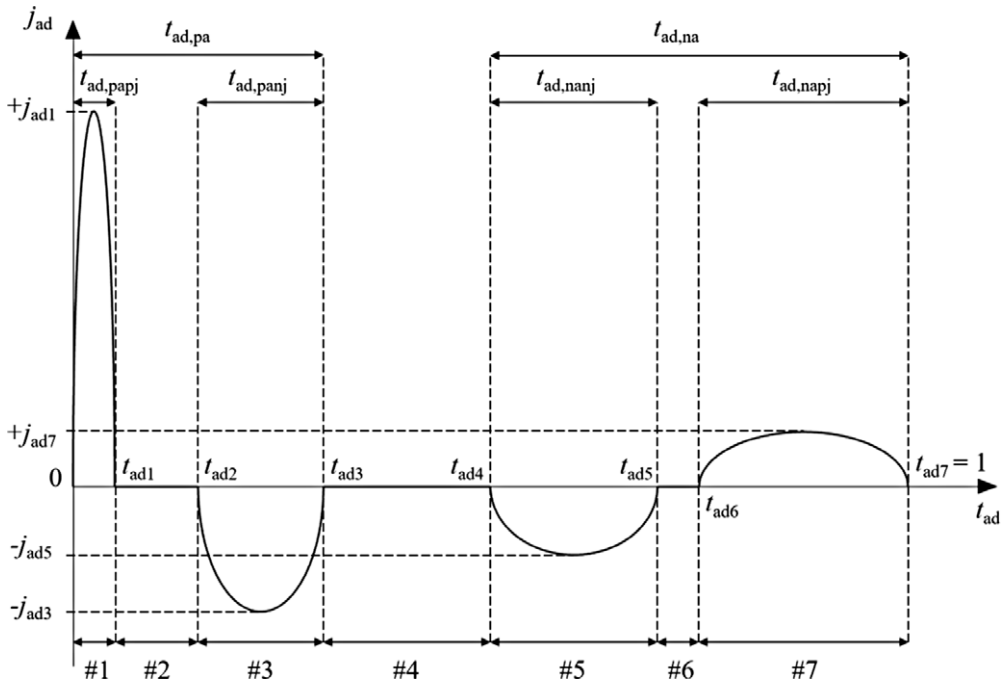


**Figure 1.** Elliptic jerk motion profile as a function of the dimensionless time  $t_{ad}$ .

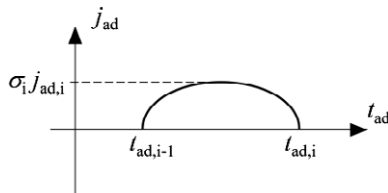


**Figure 2.** Elliptic jerk as a function of dimensionless time  $t_{ad}$  for the  $i$ th phase.

There are four phases with non-null jerk: #1, 3, #5, and #7. In these phases, the jerk profile is elliptic. The two phases with positive jerk, #1 and #7, have, respectively, maximum values of  $+j_{ad1}$  and  $+j_{ad7}$ . The two phases with negative jerk, #3 and #5, have, respectively, minimum values of  $-j_{ad3}$  and  $-j_{ad5}$ . With the hypothesis of the elliptical profile, the dimensionless jerk law is completely defined by 10 positive parameters:

- four positive jerk peak parameters:  $j_{ad1}, j_{ad3}, j_{ad5}, j_{ad7}$ ;
- six time parameters:  $t_{ad,pa}, t_{ad,na}, t_{ad,papj}, t_{ad,panj}, t_{ad,nanj}, t_{ad,napj}$ .

### 3. Analytical expression of the motion profile

#### 3.1. Expression of the jerk profile

The analytical expression of the motion profile can be derived from the representation of the semi-elliptical shape of the jerk of a generic phase shown in Fig. 2.

The parametric equation of the semi-ellipse of Fig. 2 is

$$\begin{aligned}
 j_{ad} &= \sigma_j j_{ad,i} \text{sen}(u) \\
 \cos(u) &= 1 - \frac{2(t_{ad} - t_{ad,i-1})}{t_{ad,i} - t_{ad,i-1}} \\
 \sigma_i &= \begin{cases} +1, & i = 1, 7 \\ -1, & i = 3, 5 \\ 0, & i = 2, 4, 6 \end{cases}
 \end{aligned} \tag{1}$$

where  $0 \leq u \leq \pi$ . By means of some trigonometric manipulation, we can obtain the following expression of the jerk, valid for all the phases, including the null jerk ones, for which  $\sigma_i = 0$ :

$$j_{ad}(t_{ad}) = 2\sigma_i j_{ad,i} \sqrt{\frac{t_{ad} - t_{ad,i-1}}{t_{ad,i} - t_{ad,i-1}} - \left(\frac{t_{ad} - t_{ad,i-1}}{t_{ad,i} - t_{ad,i-1}}\right)^2} \tag{2}$$

### 3.2. Expression of the acceleration profile

The expression of the acceleration profile has been found by analytical integration of Eq. (2), obtaining the following formula for the *i*th phase, for  $t_{ad,i-1} \leq t_{ad} < t_{ad,i}$ :

$$\begin{aligned}
 a_{ad}(t_{ad}) &= a_{ad,i-1} + \frac{1}{4}(t_{ad,i} - t_{ad,i-1}) \sigma_i j_{ad,i} a \cos\left(1 - 2\frac{t_{ad} - t_{ad,i-1}}{t_{ad,i} - t_{ad,i-1}}\right) + \\
 &\quad - \frac{1}{2}(t_{ad,i} - t_{ad,i-1}) \sigma_i j_{ad,i} \left(1 - 2\frac{t_{ad} - t_{ad,i-1}}{t_{ad,i} - t_{ad,i-1}}\right) \sqrt{\frac{t_{ad} - t_{ad,i-1}}{t_{ad,i} - t_{ad,i-1}} - \left(\frac{t_{ad} - t_{ad,i-1}}{t_{ad,i} - t_{ad,i-1}}\right)^2}
 \end{aligned} \tag{3}$$

where  $a_{ad,i-1}$  is the acceleration at the end of the *i* - 1th phase. In particular, for the phases with null jerk (*i* = 2, 4, 6),  $\sigma_i = 0$ , then acceleration is constant, and Eq. (3) becomes:

$$a_{ad}(t_{ad}) = a_{ad,i-1} \tag{4}$$

### 3.3. Expression of the velocity profile

The expression of the velocity profile has been found by analytical integration of Eq. (3), obtaining the following formula for the *i*th phase, for  $t_{ad,i-1} \leq t_{ad} < t_{ad,i}$ :

$$\begin{aligned}
 v_{ad}(t_{ad}) &= v_{ad,i-1} + a_{ad,i-1}(t_{ad} - t_{ad,i-1}) + \\
 &\quad - \frac{1}{8}(t_{ad,i} - t_{ad,i-1})^2 \sigma_i j_{ad,i} \left(1 - 2\frac{t_{ad} - t_{ad,i-1}}{t_{ad,i} - t_{ad,i-1}}\right) \arccos\left(1 - 2\frac{t_{ad} - t_{ad,i-1}}{t_{ad,i} - t_{ad,i-1}}\right) + \\
 &\quad + \frac{1}{4}(t_{ad,i} - t_{ad,i-1})^2 \sigma_i j_{ad,i} \sqrt{\frac{t_{ad} - t_{ad,i-1}}{t_{ad,i} - t_{ad,i-1}} - \left(\frac{t_{ad} - t_{ad,i-1}}{t_{ad,i} - t_{ad,i-1}}\right)^2} + \\
 &\quad - \frac{1}{3}(t_{ad,i} - t_{ad,i-1})^2 \sigma_i j_{ad,i} \sqrt{\left(\frac{t_{ad} - t_{ad,i-1}}{t_{ad,i} - t_{ad,i-1}} - \left(\frac{t_{ad} - t_{ad,i-1}}{t_{ad,i} - t_{ad,i-1}}\right)^2\right)^3}
 \end{aligned} \tag{5}$$

where  $v_{ad,i-1}$  is the velocity at the end of the *i* - 1th phase. In particular, for the phases with null jerk (*i* = 2, 4, 6),  $\sigma_i = 0$ , then acceleration is constant, and the velocity profile becomes:

$$v_{ad}(t_{ad}) = v_{ad,i-1} + a_{ad,i-1}(t_{ad} - t_{ad,i-1}) \tag{6}$$

### 3.4. Expression of the position profile

The expression of the velocity profile has been found by analytical integration of Eq. (5), obtaining the following formula for the  $i$ th phase, for  $t_{ad,i-1} \leq t_{ad} < t_{ad,i}$ :

$$\begin{aligned}
 s_{ad}(t_{ad}) = & s_{ad,i-1} + v_{ad,i-1}(t_{ad} - t_{ad,i-1}) + \frac{1}{2}a_{ad,i-1}(t_{ad} - t_{ad,i-1})^2 + \\
 & + \frac{5}{128}(t_{ad,i} - t_{ad,i-1})^3 \sigma_i j_{ad,i} \arccos\left(1 - 2\frac{t_{ad} - t_{ad,i-1}}{t_{ad,i} - t_{ad,i-1}}\right) + \\
 & - \frac{5}{64}(t_{ad,i} - t_{ad,i-1})^3 \sigma_i j_{ad,i} \left(1 - 2\frac{t_{ad} - t_{ad,i-1}}{t_{ad,i} - t_{ad,i-1}}\right) \sqrt{\frac{t_{ad} - t_{ad,i-1}}{t_{ad,i} - t_{ad,i-1}} - \left(\frac{t_{ad} - t_{ad,i-1}}{t_{ad,i} - t_{ad,i-1}}\right)^2} + \\
 & - \frac{1}{8}(t_{ad,i} - t_{ad,i-1})^3 \sigma_i j_{ad,i} \left(\frac{t_{ad} - t_{ad,i-1}}{t_{ad,i} - t_{ad,i-1}} - \left(\frac{t_{ad} - t_{ad,i-1}}{t_{ad,i} - t_{ad,i-1}}\right)^2\right) \arccos\left(1 - 2\frac{t_{ad} - t_{ad,i-1}}{t_{ad,i} - t_{ad,i-1}}\right) + \\
 & + \frac{1}{24}(t_{ad,i} - t_{ad,i-1})^3 \sigma_i j_{ad,i} \left(1 - 2\frac{t_{ad} - t_{ad,i-1}}{t_{ad,i} - t_{ad,i-1}}\right) \sqrt{\left(\frac{t_{ad} - t_{ad,i-1}}{t_{ad,i} - t_{ad,i-1}} - \left(\frac{t_{ad} - t_{ad,i-1}}{t_{ad,i} - t_{ad,i-1}}\right)^2\right)^3} \quad (7)
 \end{aligned}$$

where  $s_{ad,i-1}$  is the position at the end of the  $i - 1$ th phase. In particular, for the phases with null jerk ( $i = 2, 4, 6$ ),  $\sigma_i = 0$ , and the position profile becomes:

$$s_{ad}(t_{ad}) = s_{ad,i-1} + v_{ad,i-1}(t_{ad} - t_{ad,i-1}) + \frac{1}{2}a_{ad,i-1}(t_{ad} - t_{ad,i-1})^2 \quad (8)$$

### 3.5. Dependence of the motion profile parameters

As discussed in Section 2, the jerk profile is completely defined by 10 parameters, four jerk peak parameters and six time parameters. Consequently, also the acceleration, velocity, and position profiles, which are obtained by successive integrations, are defined by these 10 parameters. Nevertheless, these parameters are not independent, once these conditions are imposed:

- I. null acceleration at the end of phase #3:  $a_{ad}(t_{ad3}) = a_{ad}(t_{ad,pa}) = 0$ ;
- II. null acceleration at the end of phase #7:  $a_{ad}(t_{ad7}) = a_{ad}(1) = 0$ ;
- III. null velocity at the end of phase #7:  $v_{ad}(t_{ad7}) = v_{ad}(1) = 0$ ;
- IV. unit dimensionless position at the end of phase #7:  $s_{ad}(t_{ad7}) = s_{ad}(1) = 1$ .

Since acceleration is the integral of the jerk, conditions I and II mean that the semi-elliptical areas defined by the jerk profiles are equal for the couple of phases #1–#3, and for the couple #5–#7. The four conditions I–IV establish four equations in the 10 profile parameters, which can be used in different ways. One possible choice, which is adopted in the following of the work, is to obtain the four jerk peak parameters ( $j_{ad1}, j_{ad3}, j_{ad5}, j_{ad7}$ ) as functions of the six time parameters ( $t_{ad,pa}, t_{ad,na}, t_{ad,papj}, t_{ad,panj}, t_{ad,nanj}, t_{ad,napj}$ ). Using this approach, the equations representing the conditions I–IV have been elaborated, obtaining the following expressions of the four peak parameters as a function of the time parameters:

$$j_{ad1} = \frac{1}{c_1 + c_2 + c_3} \quad (9)$$

$$j_{ad3} = \frac{t_{ad,papj}}{t_{ad,panj}} j_{ad1} \quad (10)$$

$$j_{ad5} = c_0 \frac{t_{ad,papj}}{t_{ad,napj}} j_{ad1} \quad (11)$$

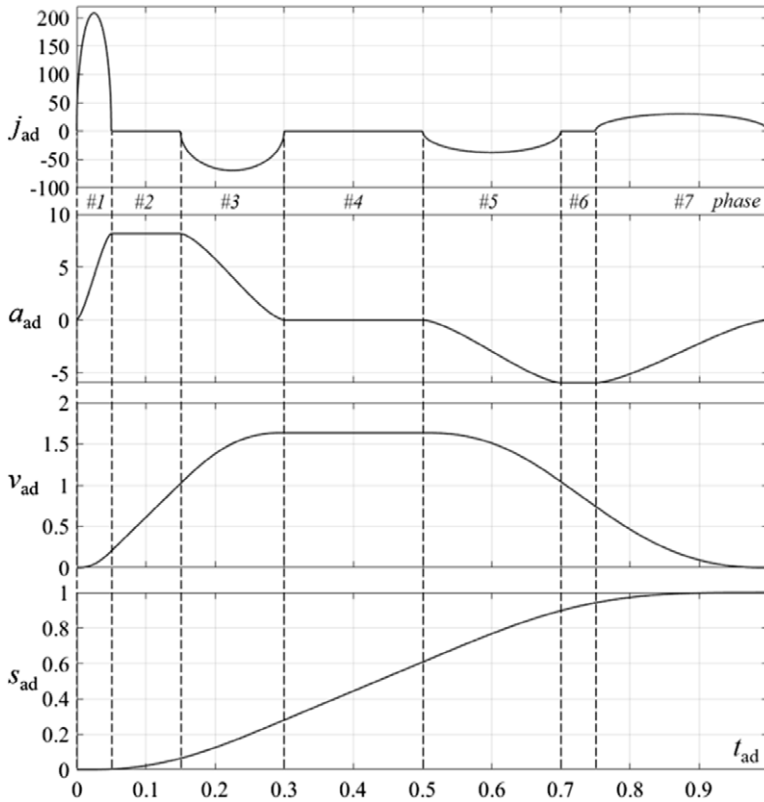


**Figure 3.** Asymmetric elliptic jerk profile: jerk, acceleration, velocity, and position profiles for  $t_{ad,pa} = 0.3$ ,  $t_{ad,na} = 0.5$ ,  $t_{ad,papj} = 0.05$ ,  $t_{ad,panj} = 0.15$ ,  $t_{ad,nanj} = 0.2$ ,  $t_{ad,napj} = 0.25$ .

$$j_{ad7} = \frac{t_{ad,nanj}}{t_{ad,napj}} j_{ad5} \tag{12}$$

where the four constants  $c_0-c_3$  are defined by the following equations:

$$c_0 = \frac{2t_{ad,pa} - t_{ad,papj} - t_{ad,panj}}{2t_{ad,na} - t_{ad,nanj} - t_{ad,napj}} \tag{13}$$

$$c_1 = \frac{\pi}{8} t_{ad,papj} t_{ad,na} (t_{ad,pa} - t_{ad,papj}) + \frac{5}{128} \pi t_{ad,papj} (t_{ad,papj}^2 - t_{ad,panj}^2) \tag{14}$$

$$c_2 = \frac{\pi}{8} t_{ad,papj} (1 - t_{ad,pa} - t_{ad,na}) (2t_{ad,pa} - t_{ad,papj} - t_{ad,panj}) \tag{15}$$

$$c_3 = \frac{\pi}{8} c_0 t_{ad,papj} t_{ad,na} (t_{ad,na} - t_{ad,napj}) + \frac{5}{128} \pi c_0 t_{ad,papj} (t_{ad,napj}^2 - t_{ad,nanj}^2) \tag{16}$$

In particular, Eq. (10) represents the ratio between the two jerk peaks in acceleration due to condition I, while Eq. (12) represents the ratio between the two jerk peaks in deceleration due to condition II. Equations (9) and (11) derive, respectively, from conditions IV and III.

For example, Fig. 3 shows the jerk, acceleration, velocity, and acceleration motion profiles obtained imposing the time parameters  $t_{ad,pa} = 0.3$ ,  $t_{ad,na} = 0.5$ ,  $t_{ad,papj} = 0.05$ ,  $t_{ad,panj} = 0.15$ ,  $t_{ad,nanj} = 0.2$ , and  $t_{ad,napj} = 0.25$ . The resulting jerk peak parameters are  $j_{ad1} = 208.07$ ,  $j_{ad3} = 69.36$ ,  $j_{ad5} = 37.83$ , and

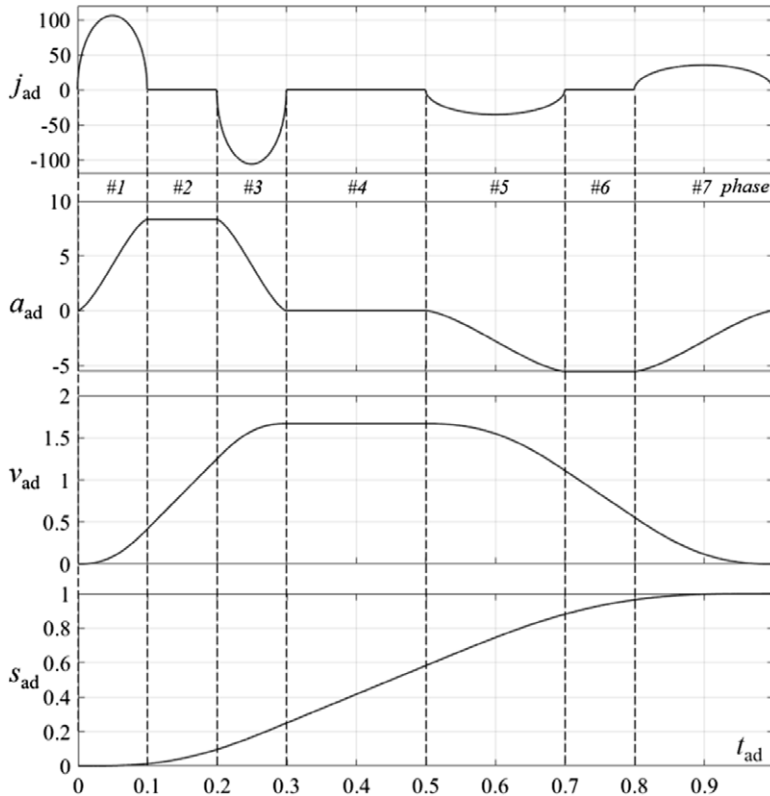


**Figure 4.** Symmetric elliptic jerk profile: jerk, acceleration, velocity, and position profiles for  $t_{ad,pa} = 0.3$ ,  $t_{ad,na} = 0.5$ ,  $t_{ad,papj} = t_{ad,panj} = 0.1$ ,  $t_{ad,nanj} = t_{ad,napj} = 0.2$ .

$j_{ad7} = 30.26$ . The dimensionless acceleration varies between a maximum of 8.17 in phase #2 and a minimum of  $-5.94$  in phase #6, while the dimensionless velocity reaches a maximum value of 1.634 in phase #4.

The maximum absolute values of dimensionless jerk, acceleration, and velocity (208.07, 8.17, 1.634) correspond to the coefficients of jerk, acceleration, and velocity, defined as follows [7]:

$$C_j = \frac{\max(|j|)}{h/T^3}, C_a = \frac{\max(|a|)}{h/T^2}, C_v = \frac{\max(|v|)}{h/T} \tag{17}$$

The jerk profile of Fig. 3 is completely asymmetric, since all the phases have different durations, and all the four jerk peaks are different. This profile is named *asymmetric elliptic jerk profile*. The maximum absolute values of acceleration and jerk are lower in deceleration (phases #5–#7) with respect to acceleration (phases #1–#3), as usual in motion control to reduce residual vibrations.

The condition of lower absolute values of acceleration and jerk in deceleration can be maintained even with a simplifying assumption, which reduces the number of profile parameters. With the hypothesis that  $t_{ad,papj} = t_{ad,panj}$  and  $t_{ad,nanj} = t_{ad,napj}$ , from Eqs. (10) and (12), it follows that  $j_{ad1} = j_{ad3}$  and  $j_{ad5} = j_{ad7}$ . Consequently, both the acceleration motion (phases #1–#3) and the deceleration motion (phases #5–#7) have symmetric acceleration profile, but can have different maximum values of acceleration and jerk. This profile is named *symmetric elliptic jerk profile*. In this case, the minimum set of parameters that define the motion profile is lower: four independent duration parameters ( $t_{ad,pa}$ ,  $t_{ad,papj} = t_{ad,panj}$ ,  $t_{ad,na}$ ,  $t_{ad,nanj} = t_{ad,napj}$ ) and two dependent peak parameters ( $j_{ad1} = j_{ad3}$  and  $j_{ad5} = j_{ad7}$ ). An example of symmetric jerk profile is shown in Fig. 4, which represents the dimensionless jerk, acceleration, velocity, and displacement for  $t_{ad,pa} = 0.3$ ,  $t_{ad,na} = 0.5$ ,  $t_{ad,papj} = t_{ad,panj} = 0.1$ , and  $t_{ad,nanj} = t_{ad,napj} = 0.2$ . The corresponding

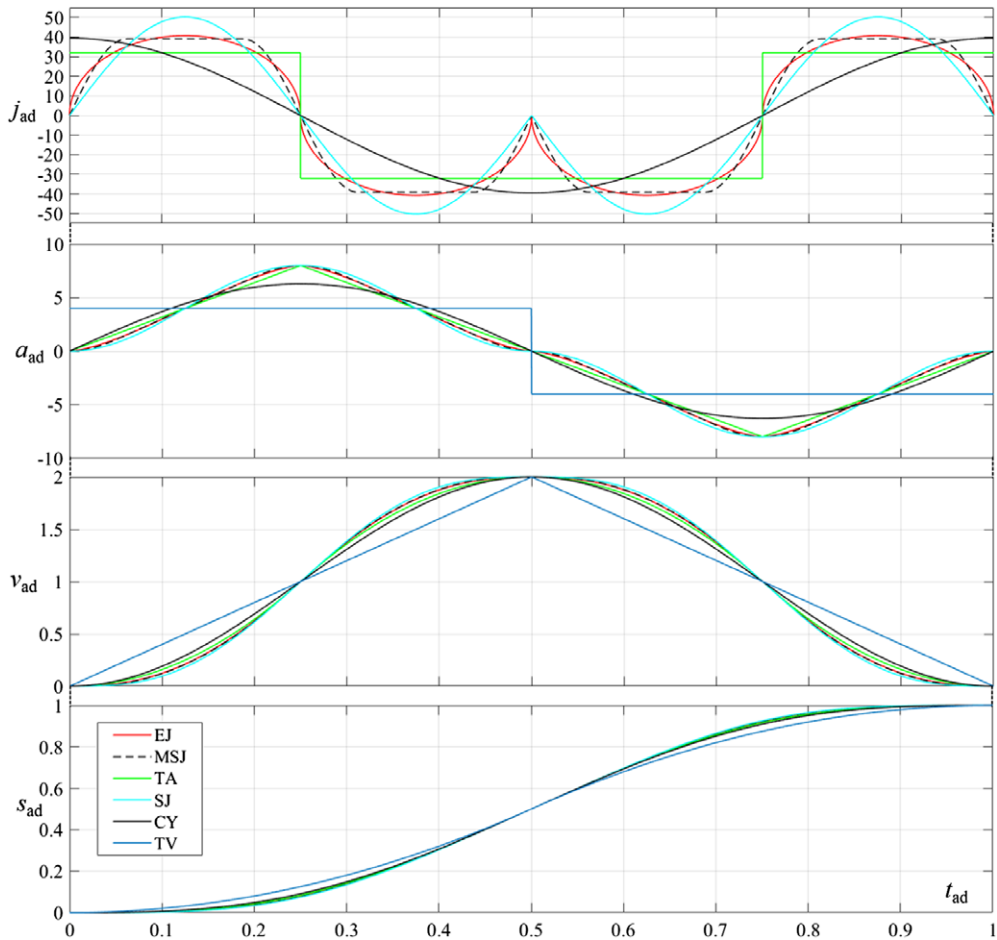


**Figure 5.** Comparison of the elliptical jerk law (EJ, red) with other motion laws: trapezoidal velocity (TV, blue), trapezoidal acceleration (TA, green), cycloidal (CY, black), sinusoidal jerk (SJ, cyan), modified sinusoidal jerk (MSJ, black dashed).

jerk peak parameters are  $j_{ad1} = j_{ad3} = 106.10$ , and  $j_{ad5} = j_{ad7} = 35.37$ . The dimensionless acceleration varies between a maximum positive of 8.33 in phase #2 and negative minimum of  $-5.56$  in phase #6, while the dimensionless velocity reaches a maximum value of 1.667 in phase #4.

#### 4. Kinematic comparison with other motion laws

In this section, the proposed elliptical jerk motion profile (EJ) is compared from a purely kinematic point of view to other geometric and trigonometric motion laws analyzed in the scientific literature, maintaining the dimensionless approach for the sake of generality. The following motion profiles are compared in Fig. 5:

- TV: trapezoidal velocity profile [7]
- TA: trapezoidal acceleration (S-curve) [7]
- CY: cycloidal profile [7]
- SJ: sinusoidal jerk profile [16]
- MSJ: modified sinusoidal jerk profile [17]

**Table I.** *Coefficients of jerk, acceleration, velocity.*

Profile	$C_j$	$C_a$	$C_v$
EJ	40.74	8	2
TV	$\infty$	4	2
TA	32.00	8	2
CY	39.48	$2\pi$	2
SJ	50.27	8	2
MSJ	39.11	8	2

The cycloidal law cannot have finite phases with null jerk. Therefore, in order to include in the comparison also the cycloidal law, for the EJ profile a null duration has been imposed for the phases with null jerk (#2, #4, #6), along with an equal duration of 1/4 for the remaining ones (#1, #3, #5, #7). With these assumptions, all the considered motion profiles are fully defined, except the MSJ profile.

In general, the MSJ profile is characterized by 15 phases [17]. In the phases #1, #3, #5, #7, #9, #11, #13, and #15 jerk is sinusoidal; in the phases #2, #6, #10, and #14 the jerk is constant; in the phases #4, #8, and #12 the jerk is null. In practice, the MSJ profile is similar to the EJ profile, but each phase with semi-elliptical jerk is replaced by a triplet of phases (sinusoidal-constant-sinusoidal). To include in the comparison the CY law, the null jerk phases of the MSJ law (#4, #8, #12) have been eliminated. The constant jerk phases cannot be eliminated; otherwise, the MSJ law becomes a SJ law. Therefore, the following assumptions are made: the duration of the phases with sinusoidal jerk is 1/16, and the duration of the phases with constant jerk is 1/8.

Table I summarizes the coefficients of jerk, acceleration, and velocity (Eq. 17) for the considered motion profiles. The influence of these coefficients is extensively debated in ref. [7]. In general, smoother trajectories present higher peaks of velocity and acceleration ( $C_v$  and  $C_a$ ). The coefficient  $C_a$  is significant since the force/torque applied by the motor is proportional to acceleration for inertial systems. On the other hand, the kinetic energy is proportional to square of velocity; therefore, it is convenient to have low values of  $C_v$ . The coefficient  $C_j$  provides an information about the jerk peaks, which influence the vibrations induced by a motion profile.

From the analysis of Fig. 5 and Table I, it is possible to summarize the following observations:

- As regards the coefficient of jerk, the SJ profile has the highest value (50.27), excluding the TV profile, which has infinite jerk, due to the acceleration discontinuities. The EJ profile has a coefficient  $C_j$  of 40.74, which is slightly higher than the ones of the CY and MSJ profiles (respectively 39.48 and 39.11). The TA profile has the lowest  $C_j$  (32.00), but has also jerk discontinuities for  $t_{ad} = 0, 0.25, 0.75,$  and  $1$ . Jerk is discontinuous also for the CY profile in  $t_{ad} = 0$ , when it varies from 0 to 39.48, and in  $t_{ad} = 1$ , when it varies from 39.48 to 0.
- As regards the coefficient of acceleration, the EJ, TA, SJ, and MSJ profiles have the same value (8), while the CY and TV laws are characterized by lower values ( $2\pi$  and 4).
- With the considered hypotheses, the coefficient of velocity has the same values for all the profiles (2).

It is possible to note that the SJ and MSJ profiles are the most qualitatively similar to the proposed EJ profile as regards the jerk shape, but the SJ as a significantly higher  $C_j$ . On the other hand, the  $C_j$  of the EJ profile is very close to the ones of the CY and MSJ laws. A significant difference between the EJ profile and the TV, TA, and CY laws is that the EJ jerk profile is continuous.

In the following section, a dynamic comparison among these motion profiles is carried out with reference to a second-order linear system.

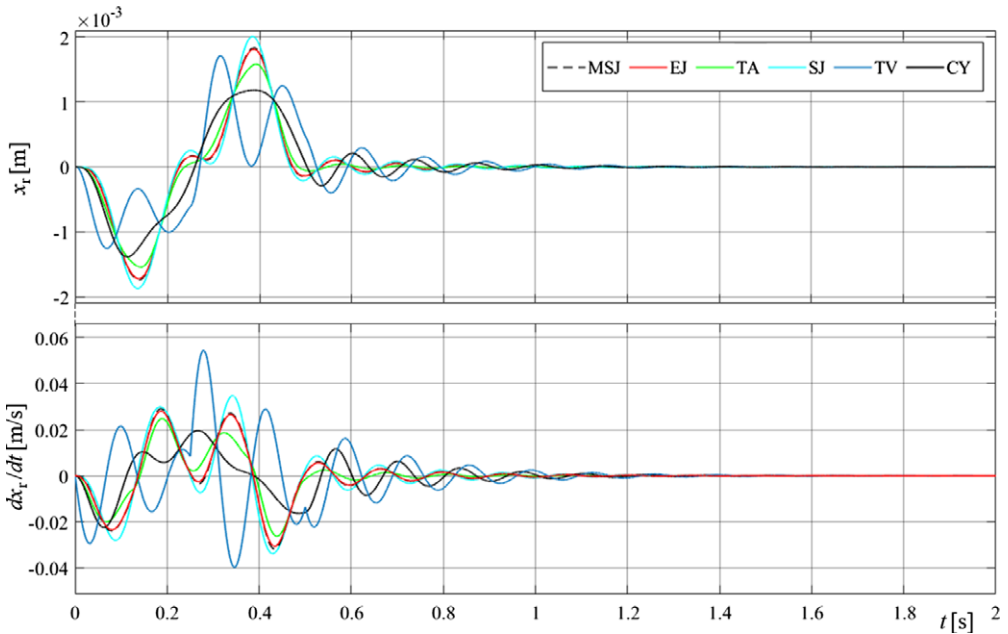


Figure 6. Dynamic comparison, case study I ( $\zeta = 0.1$ ): relative position  $x_r = x - x_d$  (top) and relative velocity  $dx_r/dt$  (bottom).

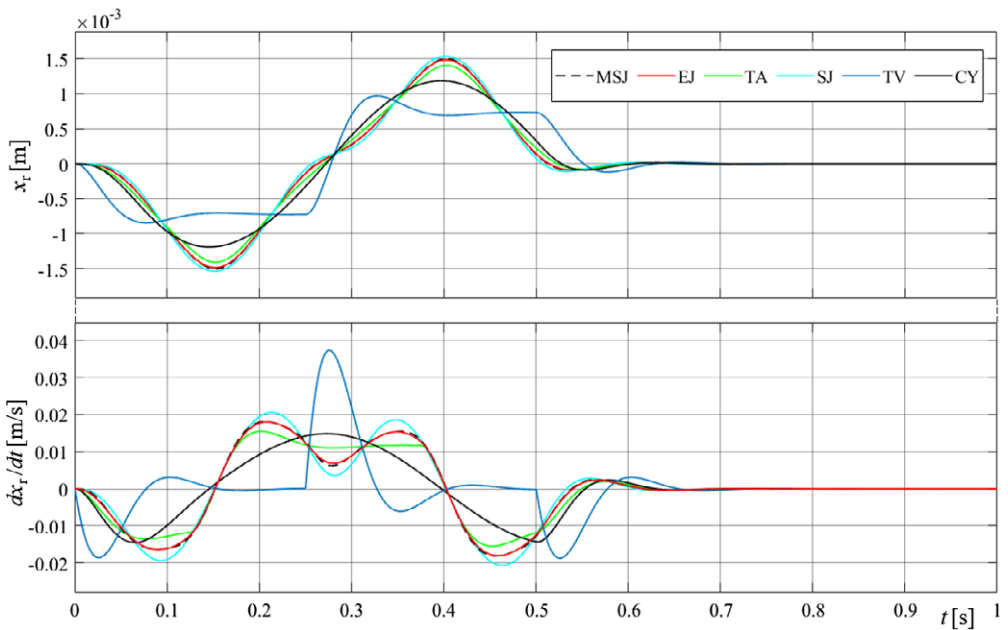
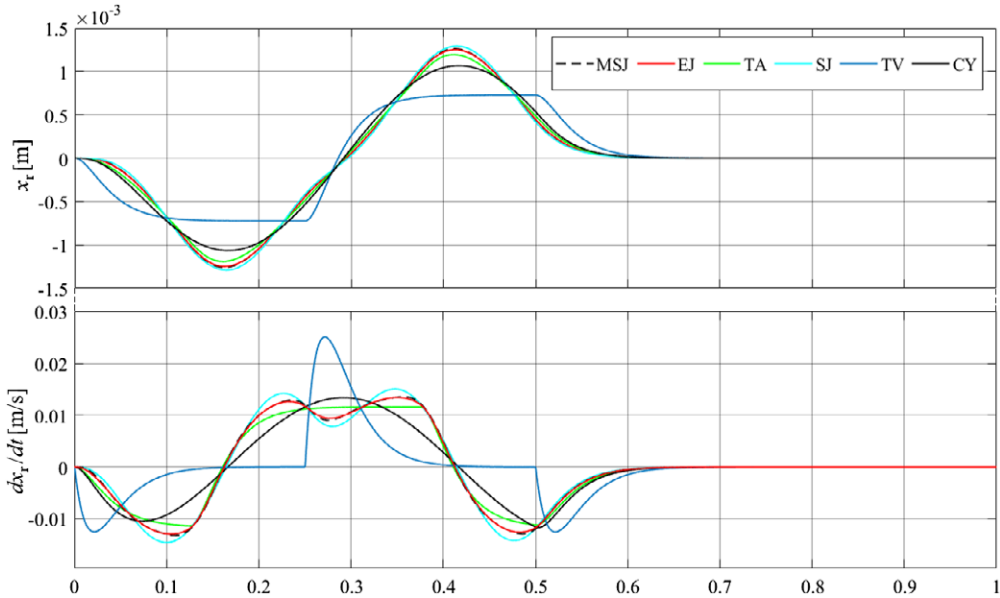


Figure 7. Dynamic comparison, case study II ( $\zeta = 0.5$ ): relative position  $x_r = x - x_d$  (top) and relative velocity  $dx_r/dt$  (bottom).



**Figure 8.** Dynamic comparison, case study III ( $\zeta = 1$ ): relative position  $x_r = x - x_d$  (top) and relative velocity  $dx_r/dt$  (bottom).

**5. Dynamic comparison with other motion laws**

For the dynamic comparison among the considered motion laws, a second-order linear system has been taken into account, characterized by the following differential equation:

$$m\ddot{x} = -k(x - x_d) - d(\dot{x} - \dot{x}_d) \tag{18}$$

This very simple linear model has been selected for the investigation since it can represent a wide variety of single-input single-output dynamic systems, such as:

- an inertia  $m$  (either translating or rotating), position-controlled by means of a PD closed-loop with proportional gain  $k$ , derivative gain  $d$ , and time-variable set-point  $x_d$ ;
- an inertia  $m$  connected in parallel by a spring with stiffness  $k$  and by a damper with coefficient  $d$  to a moving base with time-variable position  $x_d$ .

The following results are referred to a case study with  $m = 1$  kg and  $k = 2200$ N/m, considering three different levels of damping ratio  $\zeta$ : (I)  $\zeta = 0.1$  ( $d = 9.38$  Ns/m); (II)  $\zeta = 0.5$  ( $d = 46.90$  Ns/m); (III)  $\zeta = 1$  ( $d = 93.80$  Ns/m).

Six different time histories of  $x_d$  have been obtained scaling the six dimensionless profiles of Fig. 5 with a displacement  $h = 0.1$  m and a motion duration  $T = 0.5$  s. Figures 6–8 show the relative displacement  $x_r = x - x_d$  and the relative velocity  $dx_r/dt$  for the damping levels I, II, and III, comparing the vibrations deriving from the six motion profiles.

Moreover, Table II compares the six laws in terms of maximum absolute values of  $x_r$ , RMS values of  $x_r$ , settling times to within  $\pm 0.04$  mm (around 2% of the maximum relative displacement), maximum absolute values of relative velocity ( $|dx_r/dt|$ ), and maximum absolute values of relative acceleration ( $|d^2x_r/dt^2|$ ).

From the analysis of Figs. 6–8 and of Table II, it is possible to outline the following conclusions:

**Table II.** Comparison of the vibrations induced by the six considered motion laws.

Profile	max( x <sub>r</sub>  ) [mm]			RMS (x <sub>r</sub> ) [mm]			Settling time [s]			max( dx <sub>r</sub> /dt ) [m/s]			max( d <sup>2</sup> x <sub>r</sub> /dt <sup>2</sup>  ) [m/s <sup>2</sup> ]		
	I	II	III	I	II	III	I	II	III	I	II	III	I	II	III
EJ	1.81	1.48	1.25	0.493	0.450	0.403	0.715	0.570	0.571	0.031	0.018	0.013	0.972	0.585	0.379
TA	1.58	1.40	1.19	0.464	0.434	0.392	0.588	0.576	0.575	0.026	0.016	0.012	0.807	0.599	0.401
CY	1.38	1.19	1.07	0.441	0.417	0.380	0.947	0.583	0.578	0.022	0.015	0.013	0.646	0.367	0.243
SJ	2.01	1.54	1.29	0.519	0.463	0.412	0.839	0.566	0.567	0.035	0.021	0.015	1.257	0.535	0.359
MSJ	1.83	1.50	1.26	0.497	0.453	0.405	0.772	0.569	0.570	0.032	0.018	0.014	0.983	0.615	0.403
TV	1.71	0.97	0.73	0.447	0.364	0.327	1.035	0.612	0.599	0.054	0.037	0.027	2.818	3.107	3.037

- As expected, the TV profile, characterized by acceleration discontinuities and infinite jerk, induces the highest peaks of relative acceleration and velocity, and consequently the highest settling times, for all the damping levels.
- Also, the CY profile has high settling time with respect to the EJ, TA, SJ, and MSJ laws, especially in case I, with low damping; on the other hand, this profile induces the lowest peaks of relative acceleration and velocity.
- From a qualitative point of view, the dynamic responses induced by the EJ law are similar to the ones induced by the MSJ profile, for all the damping levels: as a matter of fact, in Figs. 6–8 the time histories of EJ and MSJ are nearly coincident; also the behavior related to the SJ profile is quite similar, but slightly more oscillatory.
- For all the damping levels, the maximum absolute relative displacement  $|x_r|$  of the EJ law is lower than the ones of the SJ and MSJ laws, but it is higher than the ones of the CY, TA, and TV profiles.
- The settling time of the EJ law is the second lowest in case I (lower damping), after the TA profile. In cases II and III, with higher damping, the settling times are more aligned for all the profiles, and the EJ profile is better than the TA profile. Summing the settling times in the three cases, the EJ profile is a second best after the TA law.

## 6. Conclusions and future developments

In this paper, a motion profile with elliptically shaped jerk has been proposed, presenting the analytical expressions of jerk, acceleration, velocity, and position. In dimensionless formulation, the profile is completely defined by 10 parameters: six time parameters and four jerk peak parameters. Nevertheless, imposing four necessary conditions (null acceleration at the end of phases #3 and #7, null velocity and unit displacement at the end of phase #7), the jerk parameters can be calculated as functions of the time parameters (explicit equations are presented).

Moreover, the minimum set of parameters can be reduced from six to four with the assumption that the two jerk peaks in acceleration are equal, as the two jerk peaks in deceleration (symmetric elliptic jerk profile). Also with this simplification, it is still possible to impose lower absolute values of acceleration and jerk during the deceleration, as usual in motion control to limit the residual vibrations.

The proposed law has been compared to other well-known geometric/trigonometric motion profiles: trapezoidal velocity, trapezoidal acceleration (S-curve), cycloidal, sinusoidal jerk, modified sinusoidal jerk.

First, a kinematic comparison has been carried out, discussing the coefficients of jerk, acceleration, and velocity of the considered profiles. Then, a dynamic assessment has been performed, evaluating the vibrations induced to a second-order linear system. Even if this model is very simple, it can represent adequately a wide range of real applications, such as closed-loop control of a mechatronic axis, or vibrations induced to a suspended mass by a moving base.

The results show that the elliptic jerk profile is an interesting option, since it achieves a good compromise among settling time and maximum values of relative velocity and acceleration. In particular, the performance of the elliptic jerk profile is interesting in case of high damping levels, more suitable for closed-loop position control. Regarding this application, not only the profile effectiveness using classical integer-order algorithms (PID/PD) will be assessed but also in combination with fractional-order and distributed-order controllers [18–21]; to this aim, a test bench has been prepared, and an experimental campaign is in progress.

In future work, the dynamic analysis will be extended varying continuously two parameters: (i) the damping coefficient  $\zeta$  and (ii) the nondimensional ratio between the inverse of the motion duration  $T$  and the natural frequency of the second-order system. Then, the different profiles will be compared not only in the time domain but also in the frequency domain.

Moreover, the investigation will be deepened considering not only linear systems, but extending the comparison with other motion profiles also in presence of the typical nonlinearities of real mechatronic axes with ordinary [22] and planetary [23] gears.

Finally, another research direction is the application of multi-input multi-output robotic systems. Innovative motion profiles can be used to plan end-effector point-to-point linear movements, improving different performance indexes (accuracy, energy efficiency). The study will start from simple robotic architectures, eventually statically balanced [24], arriving at flexible architectures [25].

**Author contributions.** DS conceived the elliptic jerk motion profile and obtained its analytical formulation. LB and DS designed the simulation campaign. LB, PF, and GB supervised the scientific methodology. LB and DS wrote the article.

**Financial support.** This research has been partially funded by the Interreg Project SMERF – SME Ready for the Future.

**Conflicts of interest.** The authors declare no conflicts of interest exist.

## References

- [1] A. Albu-Schäffer, S. Haddadin, C. Ott, A. Stemmer, T. Wimböck and G. Hirzinger, “The DLR lightweight robot: Design and control concepts for robots in human environments,” *Ind. Robot* **34**(5), 376–385 (2007).
- [2] L. Zhou and S. Bai, “A new approach to design of a lightweight anthropomorphic arm for service applications,” *ASME J. Mech. Robot.* **7**(3), 031001 (2015).
- [3] L. Bruzzone and R. M. Molfino, “A novel parallel robot for current microassembly applications,” *Assem. Autom.* **26**(4), 299–306 (2006).
- [4] M. Pham, B. Hazel, P. Hamelin and Z. Liu, “Vibration control of flexible joint robots using a discrete-time two-stage controller based on time-varying input shaping and delay compensation,” *ASME J. Dyn. Syst. Meas. Control* **143**(10), 101001 (2021).
- [5] A. Gasparetto, P. Boscaroli, A. Lanzutti and R. Vidoni, “Path Planning and Trajectory Planning Algorithms: A General Overview,” **In: Motion and Operation Planning of Robotic Systems, Mechanisms and Machine Science**, vol. 29 (Springer, Cham, Switzerland, 2015) pp. 3–27.
- [6] C. Lewin, “Motion control gets gradually better,” *Mach. Des.* **66**(21), 90–94 (1994).
- [7] L. Biagiotti and C. Melchiorri, *Trajectory Planning for Automatic Machines and Robots* (Springer-Verlag, Germany, 2008).
- [8] S. Macfarlane and E. A. Croft, “Jerk-bounded manipulator trajectory planning: Design for real-time applications,” *IEEE Trans. Robot. Autom.* **19**(1), 42–52 (2003).
- [9] D. M. Aspinwall, “Acceleration profiles for minimizing residual response,” *ASME J. Dyn. Syst. Meas. Control* **102**(1), 3–6 (1980).
- [10] L. Biagiotti, C. Melchiorri and L. Moriello, “Optimal trajectories for vibration reduction based on exponential filters,” *IEEE Trans. Control Syst. Technol.* **24**(2), 609–622 (2016).
- [11] G. Berselli, F. Balugani, M. Pellicciari and M. Gadaleta, “Energy-optimal motions for servo-systems: A comparison of spline interpolants and performance indexes using a CAD-based approach,” *Robot. Comput.-Integr. Manuf.* **40**, 55–65 (2016).
- [12] D. Constantinescu and E. A. Croft, “Smooth and time-optimal trajectory planning for industrial manipulators along specified paths,” *J. Robot. Syst.* **17**(5), 233–249 (2000).
- [13] K. J. Kyriakopoulos and G. N. Saridis, “Minimum Jerk Path Generation,” *Proceedings of IEEE International Conference on Robotics and Automation*, Philadelphia, PA (1988) pp. 364–369.
- [14] V. Zanutto, A. Gasparetto, A. Lanzutti, P. Boscaroli and R. Vidoni, “Experimental validation of minimum time-jerk algorithms for industrial robots,” *J. Intell. Robot. Syst. Theory Appl.* **64**, 197–219 (2011).
- [15] D. Stretti and L. Bruzzone, “Motion Profiles with Elliptic Jerk,” *Advances in Italian Mechanism Science, 4th International Conference of the IFToMM Italy, IFIT 2022, Mechanisms and Machine Science*, **MMS, 122**, (2022) pp. 45–53.
- [16] A. Valente, S. Baraldo and E. Carpanzano, “Smooth trajectory generation for industrial robots performing high precision assembly processes,” *CIRP Ann. - Manuf. Technol.* **66**, 17–20 (2017).
- [17] Y. Fang, J. Qi and J. Hu, “An approach for jerk-continuous trajectory generation of robotic manipulators with kinematical constraints,” *Mech. Mach. Theory* **153**, 103957 (2020).
- [18] I. Podlubny, “Fractional-order systems and  $PI^{\lambda}D^{\mu}$  controllers,” *IEEE Trans. Autom. Control.* **44**, 208–213 (1999).
- [19] L. Bruzzone and P. Fanghella, “Fractional-order control of a micrometric linear axis,” *J. Control Sci. Eng.* **2013**, 947428 (2013).
- [20] B. B. Jakovljević, T. B. Šekara, M. R. Rapaić and Z. D. Jeličić, “On the distributed order PID controller,” *Int J. Electron. Commun.* **79**, 94–101 (2017).
- [21] L. Bruzzone and P. Fanghella, “Comparison of  $PDD^{1/2}$  and  $PD^{\mu}$  Position Controls of a Second Order Linear System,” *Proceedings of the IASTED International Conference on Modelling, Identification and Control*, Innsbruck, Austria (2014) pp. 182–188.

- [22] F. Concli, C. Gorla, K. Stahl, B. Hoehn, K. Michaelis, H. Schultheiss and J. P. Stemplinger, “Load Independent Power Losses of Ordinary Gears: Numerical and Experimental Analysis,” *Proceedings of 5th World Tribology Congress, WTC 2013*, Turin, Italy, **2**, (2013) pp. 1243–1246.
- [23] P. Fanghella, L. Bruzzone, S. Ellero and R. Landò, “Kinematics, efficiency and dynamic balancing of a planetary gear train based on nutating bevel gears,” *Mech. Based Des. Struct. Mach.* **44**(1-2), 72–85 (2016).
- [24] L. Bruzzone and G. Bozzini, “A statically balanced SCARA-like industrial manipulator with high energetic efficiency,” *Meccanica* **46**(4), 771–784 (2011).
- [25] P. Boscariol, L. Scalera and A. Gasparetto, “Nonlinear control of multibody flexible mechanisms: A model-free approach,” *Appl. Sci.* **11**(3), 1082 (2021).